

Solution structure of crotamine, a Na⁺ channel affecting toxin from *Crotalus durissus terrificus* venom

Giuseppe Nicastro^{1,2}, Lorella Franzoni¹, Cesira de Chiara¹, Adriana C. Mancin³, José R. Giglio³ and Alberto Spisni¹

¹Department of Experimental Medicine, Section of Chemistry and Structural Biochemistry, University of Parma, Italy;

²Centro Interfacoltà Misure, University of Parma, Italy; ³Department of Biochemistry and Immunology, University of São Paulo, Brazil

Crotamine is a component of the venom of the snake *Crotalus durissus terrificus* and it belongs to the myotoxin protein family. It is a 42 amino acid toxin cross-linked by three disulfide bridges and characterized by a mild toxicity (LD₅₀ = 820 µg per 25 g body weight, i.p. injection) when compared to other members of the same family. Nonetheless, it possesses a wide spectrum of biological functions. In fact, besides being able to specifically modify voltage-sensitive Na⁺ channel, it has been suggested to exhibit analgesic activity and to be myonecrotic. Here we report its solution structure determined by proton NMR spectroscopy. The secondary structure comprises a short N-terminal α-helix and a small antiparallel triple-stranded β-sheet arranged in an αβ₁β₂β₃ topology never found among toxins active on ion

channels. Interestingly, some scorpion toxins characterized by a biological activity on Na⁺ channels similar to the one reported for crotamine, exhibit an α/β fold, though with a β₁αβ₂β₃ topology.

In addition, as the antibacterial β-defensins, crotamine interacts with lipid membranes. A comparison of crotamine with human β-defensins shows a similar fold and a comparable net positive potential surface.

To the best of our knowledge, this is the first report on the structure of a toxin from snake venom active on Na⁺ channel.

Keywords: β-defensin; myotoxin; NMR; scorpion toxin; structure.

Despite the fact that Na⁺ channels are affected by a large variety of toxins from arthropods, coelenterates, microorganisms, fish and plants, they are seldom the targets of toxins from snake venom [1]. One exception is crotamine (Crt), a protein of 42 amino acids present in the venom of *Crotalus durissus terrificus* [2,3] and characterized by a wide spectrum of biological activities. This toxin, in fact, has been known for a long time to be able to induce membrane depolarization dependent muscle contractions by increasing the Na⁺ permeability of skeletal muscle membranes [4–9] and to affect, in an allosteric fashion, the action of other Na⁺ channel neurotoxins (i.e. tetrodotoxin, veratridine, batrachotoxin and grayanotoxin) [4,5,7–10]. In addition, while loose patch-clamp recording of macroscopic sodium currents in frog skeletal muscle has revealed that Crt inhibits the inactivation of the Na⁺ channel in a fashion similar to that of scorpion α-toxins [11], other experiments have shown that, at low doses, it has an analgesic activity involving both central

and peripheral mechanisms [12]. Moreover, Crt actively interacts with lipid membranes being able to form vacuoles and exhibiting myonecrotic activity [13,14].

Crt belongs to a family of small basic rattlesnake venom myotoxins that includes myotoxin a [15], peptide C [16], myotoxin I and II [17] and the CAM toxin [18]. They exhibit high primary sequence identity (Fig. 1) and, in addition, they are antigenically related [19]. However, when compared to the other members of the family, Crt exhibits a reduced toxicity (intraperitoneal injection LD₅₀ = 820 µg per 25 g body weight) [12]. Interestingly, the three-dimensional (3D) structure of all these toxins is yet unknown.

As for Crt, the absence of direct binding studies using a radioactively labelled toxin, as well as the lack of structural information, has strongly hampered the possibility either to identify the receptor site on the Na⁺ channel or to suggest some precise hypothesis about the molecular mechanisms associated with the multiplicity of its biological functions.

In the attempt to answer these questions, we have been prompted to solve its 3D solution structure. The results reveal that Crt is characterized by an αβ₁β₂β₃ structural topology, so far, never found in toxins active on ion channels. This observation and the high sequence identity with other myotoxins suggest that the 3D fold of Crt may represent a canonical structure of that protein family.

In addition, we show that both its fold and potential surface partially resemble the structural features of the antimammalian scorpion α-neurotoxins and of the human antibacterial β-defensins with which Crt shares some biological properties.

Correspondence to A. Spisni, Department of Experimental Medicine, Section of Chemistry and Structural Biochemistry, University of Parma, Via Volturmo, 39, 43100 Parma, Italy.

E-mail: aspin@unipr.it

Abbreviations: AaHII, scorpion toxin from *Androctonus australis* Hector II; Crt, crotamine.

Note: The atomic coordinates of crotamine have been deposited in the RCSB Protein Data Bank, with accession code 1H5O.

(Received 27 November 2002, revised 8 February 2003, accepted 10 March 2003)

using well defined geminal H_{β} - H_{β} connectivities. NOEs were classified as strong, medium, weak and very-weak, corresponding to interproton upper distance restraints of 3.0 Å, 4.0 Å, 5.0 Å and 6.0 Å, respectively. Upper distance restraints involving nonstereo-specifically assigned methylene, aromatic, and methyl protons were replaced by appropriate pseudoatoms [27]. The long- and medium-range restraints involving side-chains protons were further relaxed by an additional 0.5 Å to account for internal motions.

NH - C_{α} - H coupling constants were estimated in DQF-COSY spectrum from the measurements of extrema separations in dispersive and absorptive plots of rows through cross peaks [28]. In this experiment, the digital resolution after zero-filling along $F2$ was 0.56 Hz per point. A total of 24 ϕ angle restraints were derived from the $^3J_{NH-\alpha H}$ coupling constants using the Karplus relation [29], and were used for structure calculations with an allowed tolerance of $\pm 30^\circ$.

Disulfide bonds between cysteine residues 4–36, 11–30, 18–37, identified on the basis of the known disulfide pairing pattern of the myotoxin a [15], were defined as covalent linkages and introduced after the first cycle of structure calculation. All peptide bonds were constrained to the *trans* position ($\Omega = 180^\circ$) with the exception of the one between Leu19 and Pro20 that was constrained to the *cis* position ($\Omega = 0^\circ$), as indicated by the presence of characteristic NOEs.

Structures were computed using the simulated annealing method [30] in the NMR-Refine module of the INSIGHTII package (MSI Molecular Simulations Inc., San Diego, CA, USA). The 26 best structures were further refined using a dynamic simulated annealing protocol. Final minimizations were performed with full Consistent Valence Force Field (CVFF), to a maximum derivative of $0.001 \text{ kcal}\cdot\text{Å}^{-1}$. Solvation effects were simulated by using a distance-dependent dielectric constant.

The Crt ensemble was inspected by the program INSIGHT-II and analyzed by PROCHECK-NMR [31]. The program MOLMOL [32] was used to analyze the structures in terms of rmsd values, hydrogen bonds, regular secondary structures, solvent-accessible surface areas, angular order parameters, and electrostatic potential.

Results and discussion

Circular dichroism

The far-UV CD spectrum of Crt at pH 4.0 shows, as for many toxins [33], two main bands at 197 nm (positive) and at 207 nm (negative) together with a less intense positive band at approximately 222 nm (Fig. 2). This last spectral feature, generally unusual for globular proteins, is shared by a number of other proteins, including toxins such as cobratoxin, erabutoxin b, myotoxins and α -neurotoxins [34,35].

The presence of a positive band at approximately 195 nm and of a negative one in the range 210–215 nm, usually indicates a dominant antiparallel β -sheet folding [33]. In this case, however, the observed blue shift to 207 nm of the negative band suggests the presence of some helical contribution.

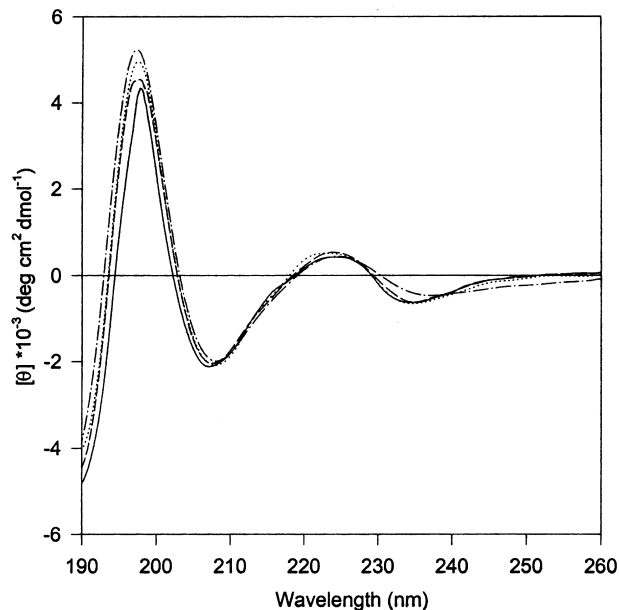


Fig. 2. CD spectra of crotamine at 20 °C in 3 mM potassium phosphate buffer as a function of various trifluoroethanol concentrations (% v/v, pH \approx 4). Solid line, 0%; dashed line, 30%; dotted line, 50%; dashed-dotted line, 90%.

The band in the region 221–231 nm is consistent with a B_b transition arising from the Trp residues and/or with the $L_a(0 \rightarrow 1)$ transition associated with the Tyr residues [35]. Nonetheless, we cannot exclude the possibility that the band originates as a contribution from the disulfide bridges [36].

As for a large number of toxins [33], probably because of the constraints imposed by the disulfide bonds, we found that the secondary structure of Crt is independent on pH in the range 3.7–9.0 (data not shown), thus confirming previous results obtained by SAXS [37,38] and ORD [39].

The titration with trifluoroethanol performed at pH 4.0 (Fig. 2), shows that the CD spectrum remains almost unchanged up to 90% trifluoroethanol. Only at the highest cosolvent concentration did we observe a minor perturbation of the toxin secondary structure.

NMR data

A number of studies using polyacrilamide gel electrophoresis [40] and SAXS [37,38] have indicated that Crt in aqueous solution may dimerize or, more in general, aggregate. Indeed, the NMR proton spectra obtained at a protein concentration of approximately 1 mM in water were indicative of aggregation (data not shown). Recognizing that trifluoroethanol, besides stabilizing secondary structures is able to disrupt aggregates [41–43] and having verified by CD spectroscopy that moderately low concentrations of trifluoroethanol do not induce any significant alteration of the toxin secondary structure, the NMR experiments have been carried out in H_2O /trifluoroethanol (70 : 30, v/v) in order to shift the dimerization equilibrium towards the monomeric form [44]. Under these experimental conditions, we could observe only a few and very weak

additional peaks that did not interfere with spectra analysis, which differed from previous reports for both Crt [45] and myotoxin a [46].

The sequence-specific resonance assignment of Crt has been carried out according to the sequential assignment procedure [27]. The combined analysis of the fingerprint regions of the TOCSY and DQF-COSY spectra, recorded at 35 °C, revealed all the expected NH-C α H cross-peaks. The sequential connectivities were obtained from the NOESY spectrum recorded with a mixing time of 100 ms. Spectra recorded at different temperatures were also used to confirm assignments in cases of peak overlap or proximity to the water resonance.

A comparison of amide and α -protons chemical shifts of Crt with respect to the corresponding ones reported for myotoxin a in water [46] revealed a large identity (within ± 0.3 p.p.m.) for almost all the residues. This finding is not surprising if we keep in mind that the two molecules share 39 out of the 42 amino acids. Furthermore this indicates that the amount of cosolvent used did not affect the protein structure. A major difference was observed only for Phe25 α H and Lys38 NH. As for residue 25, the reason could be

that while myotoxin a carries a leucine, in Crt there is a phenylalanine that, in addition, could be also responsible for the difference in the Lys38 NH chemical shifts. In fact, in the structures of Crt, the side-chain of Phe 25 is close enough to the amide proton of Lys38 to induce a ring current effect.

Description of the toxin structure and potential surface

The characteristic NOE connectivities, reported in Fig. 3A, and the analysis of the ϕ and ψ angle distribution allowed the identification of the type and boundaries of the secondary structure elements. Crt consists of three antiparallel β -strands (involving residues 9–12, 24–25, 35–38), one α -helix (residues 3–7), and three β -turns (residues 13–16, 27–30 and 31–34). The first β -strand is connected to the second one by a long and solvent exposed loop, Pro13–Ser23. The loop comprises the first turn which, based on the ϕ/ψ angles, can be classified as a distorted type-I β -turn. The second and third β -strands are connected by a loop presenting two consecutive β -turns of which the first can be classified as a type-VIII and the second one as a type-I. The +2 x , -1 topology [47] of the triple-stranded antiparallel β -sheet was

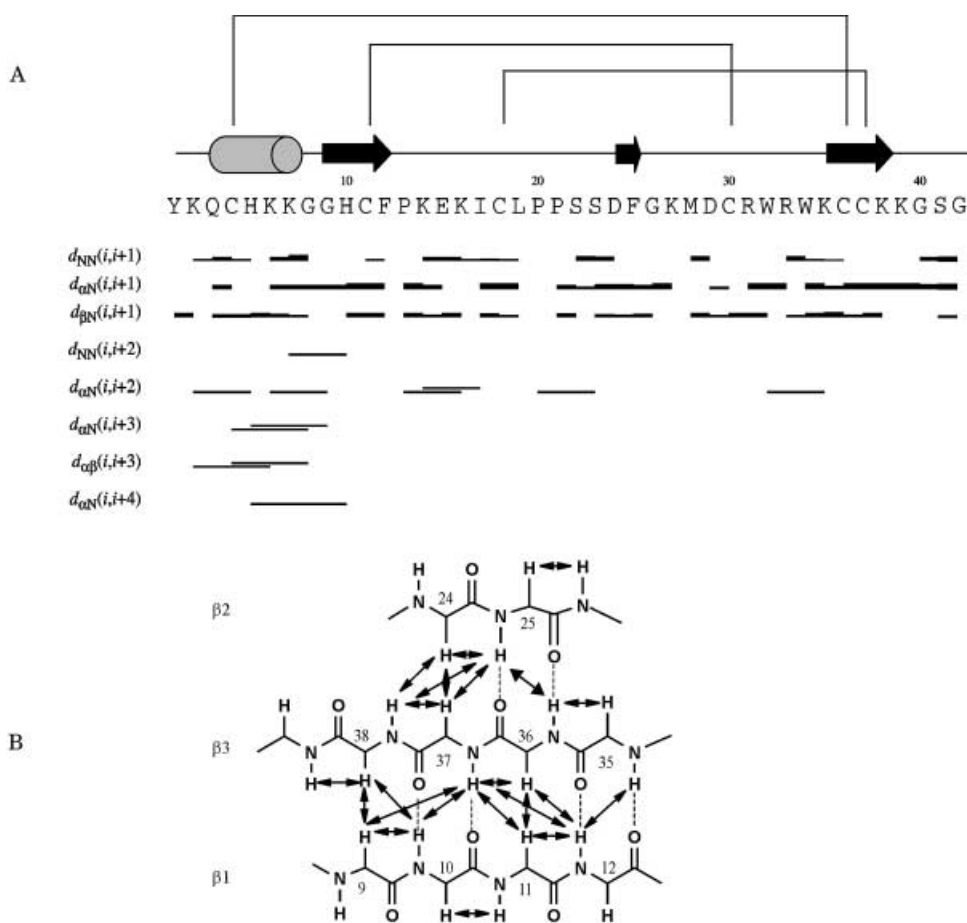


Fig. 3. Summary of data used in the determination of the secondary structure of crotamine. (A) Primary sequence of Crt with the sequential and medium-range NOE pattern. For sequential connectivities, the thickness of the bars indicates the NOE intensities; medium-range NOEs are identified by lines connecting the two-coupled residues. (B) Schematic representation of Crt secondary structure showing the three antiparallel β -strands together with the intra- and interstrand NOE connectivities (double-arrow lines) defining the topology of the β sheet. Broken lines indicate the expected intrachain hydrogen bonds.

identified based on the presence of the characteristic intra- and interstrand NOEs (Fig. 3B). As a result, the toxin shows an $\alpha\beta_1\beta_2\beta_3$ topology where both the first and the second strands run antiparallel to the third one. The β -sheet is twisted in a right-handed fashion and it is stabilized by four hydrogen bonds between strands β_1 and β_3 , involving residues 10–37 and 12–35, and by two hydrogen bonds between strands β_2 and β_3 , involving residues 25–36. The hydrogen bonds were identified in the final structures even though no constraints for those interactions had been introduced during the structure calculation.

As for the three disulfide bridges, while Cys4–Cys36 and Cys18–Cys37 connect the strand β_3 with the α -helix and the first loop (Pro13–Ser23), respectively, Cys11–Cys30 connects β_1 with the second loop (Gly26–Trp34), Fig. 3A.

Among the three prolines, Pro13 and Pro21 form peptide bonds in *trans* conformation, as inferred by the presence of strong $d_{\alpha\delta}(i, i + 1)$ connectivities. In the case of Pro20, instead, a strong NOE between Leu19 and Pro20 α H protons indicates that the peptide bond is in *cis* conformation, thus creating a kink in the polypeptide chain.

A final set of restraints consisting of 580 non-redundant interproton distances and 24 ϕ dihedral angles was derived from spectral analysis, Table 1. A plot showing the total number of NOE-derived interproton distance restraints for each residue is given in Fig. 4 (top).

A total of 50 structures was determined and the best 26 were selected (Fig. 5) as they satisfy the criteria of systematic

Table 1. Structural statistics of the 26 selected solution structures of crotamine.

Restraints statistics	Number
meaningful distance restraints	580
intra-residual	224
inter-residual	356
sequential	173
medium range	54
<i>i, i + 2</i>	29
<i>i, i + 3</i>	21
<i>i, i + 4</i>	4
long-range	129
ϕ dihedral angles	24
Mean rmsd from idealized covalent geometry	
bonds (Å)	0.002
angles (°)	0.90
Ramachandran angle distribution	%
most favoured regions	63.6
additional allowed regions	30.3
generously allowed regions	6.1
disallowed regions	0
rmsd (Å) from the mean structure	(Å)
backbone (residues 2–39)	0.91 ± 0.15
heavy atoms (residues 2–39)	1.47 ± 0.15
backbone (residues 3–7, 9–12, 24–25, 35–38)	0.44 ± 0.06
heavy atoms (residues 3–7, 9–12, 24–25, 35–38)	1.03 ± 0.10
backbone (residues 9–12, 24–25, 35–38)	0.39 ± 0.09
heavy atoms (residues 9–12, 24–25, 35–38)	0.99 ± 0.15
backbone (residues 3–7)	0.19 ± 0.10
heavy atoms (residues 3–7)	0.81 ± 0.18

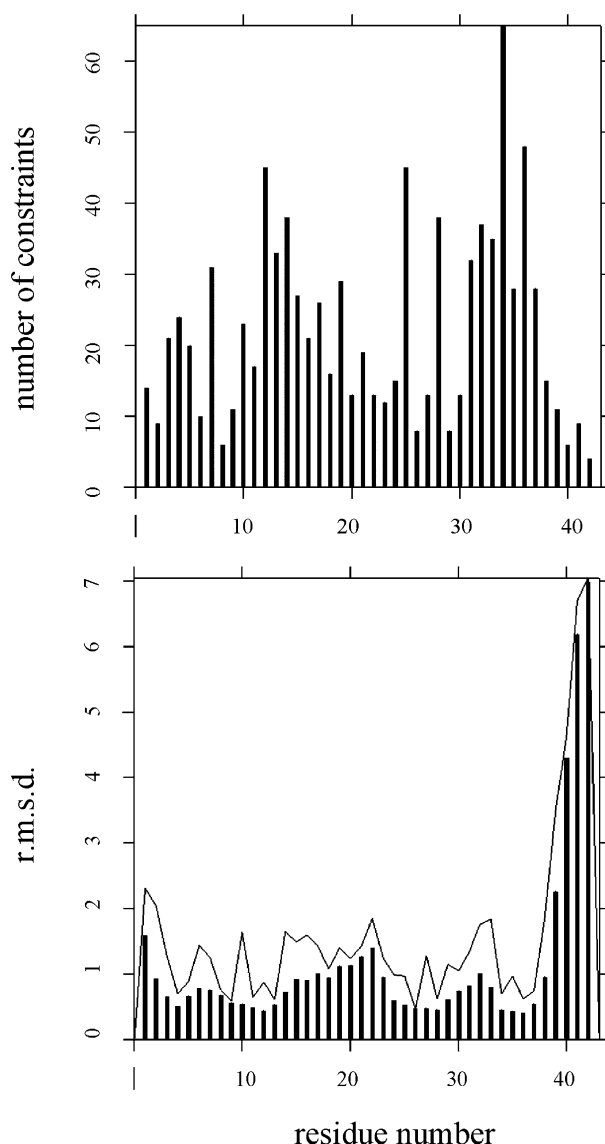


Fig. 4. Parameters characterizing the 26 structures of crotamine, plotted as a function of residue number. Top: number of interproton distance constraints; bottom: rmsd values for backbone (bars) and heavy (line) atoms.

residual distance violations not greater than 0.5 Å and dihedral violations not more than 5°. As already suggested by previous studies [37,38] the molecule has a flat shape and the molecular plane corresponds approximately to the triple-stranded β -sheet with the short α -helix packed against the sheet.

The superposition of the 26 selected structures over residues 2–39 (Fig. 5), showed a global rmsd, with respect to the mean structure, of 0.91 ± 0.15 Å for backbone atoms and 1.47 ± 0.15 Å for all heavy atoms. Further details of the statistics of the NMR models are listed in Table 1. Analysis of the Ramachandran plot, performed with the PROCHECK_NMR program [31], shows that 64% of the residues lie in the most favoured regions, 30% in the additional allowed regions and 6% in the generously

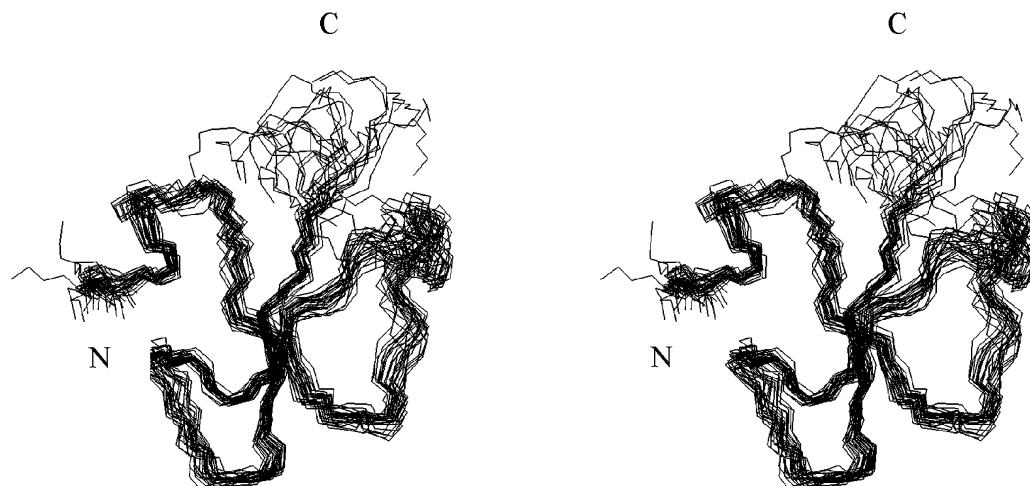


Fig. 5. Solution structure of crotamine. Stereo view of the 26 NMR models superimposed over the backbone atoms of residues 2–39.

allowed regions. The low mean rmsd values from the idealized covalent bond (0.002 Å) and covalent angles (0.90°) indicate the absence of stereochemical distortions.

An assessment of the local variability of backbone and heavy atoms positions is provided by the histogram of the rmsd (Fig. 4, bottom). As expected, the regions presenting elements of regular secondary structure are better defined. In fact, the backbone rmsd value restricted to residues 3–7, 9–12, 24–25 and 35–38, is 0.44 ± 0.06 Å with respect to the mean structure and the corresponding ϕ and ψ order parameters, $S(\phi)$ and $S(\psi)$, are generally 1.

The disulfide bonds show a certain conformational disorder exhibiting two sets of conformations corresponding to $\chi_3 = \pm 90^\circ$. This disorder is consistent with the lack of specific $H\beta_1$ - $H\beta_3$ NOEs across the bond.

The segment Ile17–Ser23 and the C-terminal region (residues Gly40–Gly42) exhibit a poor backbone definition (Fig. 5) due to the absence of assignable long-range NOEs.

Figure 6A,B shows a representation of the electrostatic potential associated with the solvent-accessible surface of Crt and evidences the presence of a large positive patch (blue) with only three negative small regions (red).

In addition, it is interesting to note that Lys35, out of the nine Lys residues, is not exposed to the solvent and its $H\zeta$ is within H-bonded salt-bridge distance to the Asp24 carboxyl oxygen.

Comparison with scorpion α -toxins and β -defensins

The NMR-derived models show that Crt exhibits an α/β motif, Fig. 7A, a structural feature observed not only in other toxins that affect ion channels, such as the α - and β -toxins from scorpion venom (Fig. 7B) but also in non-related proteins, such as β -defensins (Fig. 7C) and thionins [48–55].

As for the scorpion α - and β -toxins, their biological activity consists of the ability to modify the Na^+ permeability by modulating the gating of the Na^+ channel. In particular, while α -toxins slow or inhibit the sodium current inactivation [56,57], β -toxins shift the activation voltage to more negative potentials [58]. Studies on the α -toxin present

in the venom of the scorpion *Leiurus quinquestratus* suggested that the binding site for that toxin overlaps to a considerable extent to the one for Crt [7]. The hypothesis of a common binding site [7] has been further supported by the observation that Crt, similarly to scorpion α -toxins, enhances the depolarizing effect of the lipid soluble toxins veratrine, batrachotoxin and grayanotoxin [8]. Indeed, recent studies on the inactivation kinetics of the Na^+ current [11] have evidenced that Crt and scorpion α -toxins act in a very similar fashion.

Based on these observations and looking for the presence of common structural determinants that could justify the observed functional similarities, we have compared Crt with the most representative member of the scorpion α -toxins family, the antimammalian AaHII [57,60] (PDB accession no. 1PTX).

Despite the low sequence homology and a distinct sequential arrangement of the secondary structure elements ($\alpha\beta_1\beta_2\beta_3$ for Crt vs. $\beta_1\alpha\beta_2\beta_3$ in the case of AaHII), the global fold of the two toxins appears quite similar, Fig. 7A,B. Crt could be considered a structurally simplified form of AaHII, with a truncated N-terminal portion of the α -helix, shorter β -strands and the lack of the relatively long C-terminal region, thus suggesting a possible common ancestral origin.

To compare the two toxins better, Crt and AaHII have been aligned with respect to their secondary structure elements, i.e. β_2 of Crt with β_1 of AaHII, the two α -helices with respect to each other, β_1 and β_3 of Crt with β_2 and β_3 of AaHII, respectively, Fig. 8. As a result, introducing some gaps in order to maximize similarities among residues, a certain degree of homology in the primary sequence becomes apparent.

In particular, it is worthwhile to point out that Tyr1 of Crt corresponds to Tyr21 in AaHII, located in the first turn of the helix and Cys4 of Crt, connecting the α -helix to the β_3 strand, corresponds to Cys26 of AaHII that, similarly, connects the α -helix to the strand β_3 .

In Crt, Gly8 is located between the helix and strand β_1 and has its correspondent in Gly31, belonging to the loop that connects the α -helix to strand β_2 of AaHII. This can be

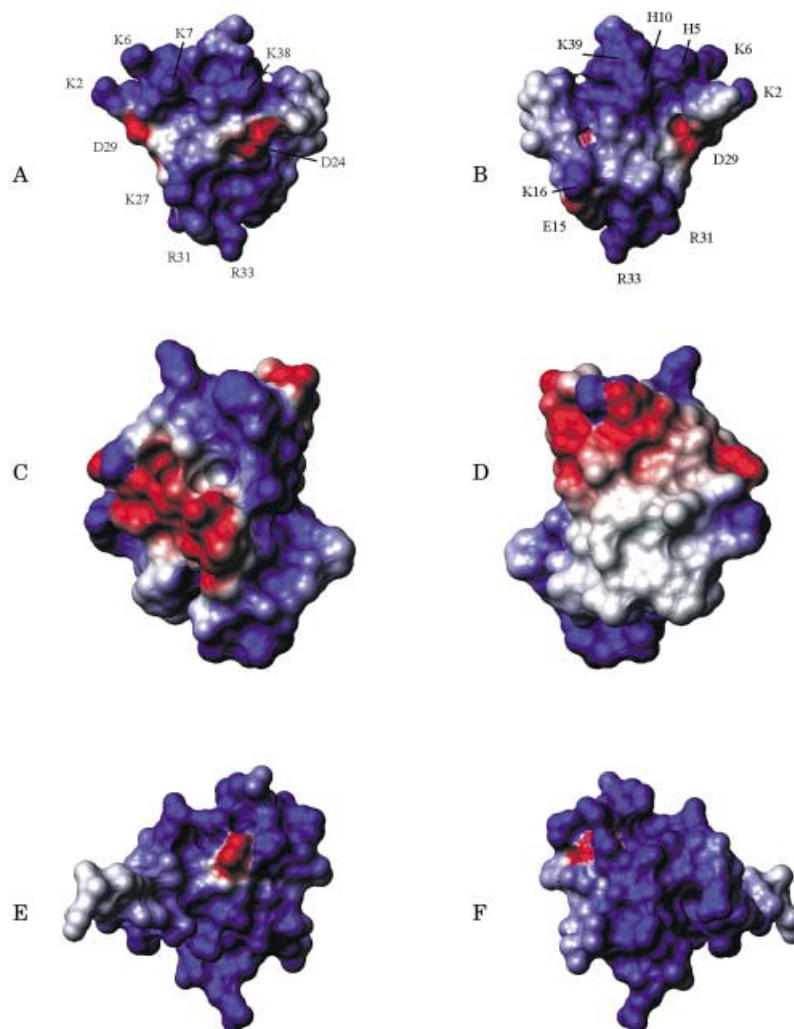


Fig. 6. Comparison of the electrostatic potential surface between crotamine (A and B), AaHII (PDB accession no. 1PTX) (C and D) and HBD3 (PDB accession no. 1KJ6) (E and F). Positively and negatively charged regions are coloured in blue and red, respectively. The orientation in A, C and E is the same as in Fig. 7. The views in B, D and F result from a 180° rotation of A, C and E around their vertical axis.

considered an example of structural simplification. In fact, while in Crt a single glycine residue forms this junction, in AaHII the connection is composed of three residues, Leu29–Gly31.

Analyzing the strand β_1 of Crt, we find that Gly9, His10, and Cys11 have their counterpart in residues Gly34, Tyr35 and Cys36 in the strand β_2 of AaHII. Noteworthy, the residues Gly9–Cys11 in Crt and Gly34–Cys36 in AaHII form a consensus sequence, GXC, that, in scorpion toxins as well as in β -defensins and thionins, appears to be related to a specific structural requirement [49]. In fact, it has been suggested that glycine must be conserved in the α/β motif due to steric hindrance between the helix and the sheet and it is essential for a correct folding [49,50].

The Phe12 residue, located at the end of strand β_1 of Crt, presents its counterpart in Trp38 similarly located at the end of strand β_2 of AaHII. Interestingly, chemical modifications of scorpion α -toxins have demonstrated that the aromatic residues Trp38 and Tyr21 (corresponding to Tyr1 in Crt), may have an important role for their toxicity and efficiency in binding to Na^+ channels [61,62].

Asp24 and Phe25, located in strand β_2 of Crt, have their structural correspondent in Asp3 and Tyr5; the latter residue is highly conserved among scorpion α -toxins [63] and it is arranged in a 'herringbone' fashion in the aromatic cluster present in the β_1 strand of AaHII [59,60].

The disulfide bridge Cys11–Cys30 of Crt, that anchors the strand β_1 to the loop Gly26–Trp34, has its correspondent in disulfide Cys36–Cys16 of AaHII that, similarly, connects the topologically equivalent β_2 strand to the loop Tyr5–Arg18. Overall, it is noteworthy that out of the six cysteine residues present in Crt, five match the ones in AaHII.

Besides all these similarities, the alignment also reveals that the residues responsible for the formation of the hydrophobic patch, common to the scorpion toxins, are not structurally conserved in Crt. However, in the vicinity of the Crt hydrophobic patch we find the salt-bridge Asp24–Lys35, similar to that observed in AaHII, ion-pair Glu32–Lys50, and in other scorpion α -toxins.

Large regions of the Crt and AaHII surface are characterized by a positive electrostatic potential (Fig. 6A–D). Clearly, this feature is more pronounced for Crt that

Recently, much attention has been given to the human basic antimicrobial polypeptides β -defensins [70,71]. Interestingly, they display a 3D fold similar to Crt (Fig. 7A,C) and comparable potential surface (Fig. 6A, B,E,F). The superposition of the C α -trace atoms of the secondary structure regions of the three human β -defensins HBD1, HBD2 and HBD3, residues 3–8, 10–13, 23–24, 33–36, for HBD1 (PDB 1IJU), residues 6–11, 13–16, 26–27, 36–39, for HBD2 (PDB 1FD3) and residues 10–13, 17–19, 28–29, 39–42 for HBD3 (PDB 1KJ6), onto the corresponding ones of the Crt solution structure, yields average rmsd values of 0.9, 1.0 and 1.5 Å, respectively. Although β -defensins and Crt show a relatively low sequence identity (30%) (Fig. 1), the sequence alignment reveals the conservation of the elements of secondary structure as well as of residues responsible for the formation of the β -defensin fold, such as the 6 Cys residues, the Gly residues 8, 9, 26 and Pro20 [51].

It has been proposed that β -defensins exhibit their activity by disrupting the bacterial membranes as a result of polar interactions and oligomer formation [51,52,54]. This antimicrobial activity as well as the ability to form dimers in solution appears to be directly proportional to their net positive surface charge [51,52,54].

Considering that, similarly to these proteins, Crt exhibits a highly positive potential surface (Fig. 6A,B,E,F) and a clear tendency to form aggregates [37,38,40], we can hypothesize that, as the β -defensins, it can interact electrostatically with the negative surface of the membranes inducing the formation of gaps through which ions and/or other molecules can move. Indeed, such a possibility might justify the observed Crt myonecrotic activity mediated by the formation of vacuoles [13,14].

In conclusion, Crt is an example where structural homologies with proteins deriving from different species provide the key to interpret its complex biological activity.

Indeed, the presence of the α/β scaffold and the existence of a surface characterized by a positive electrostatic potential seem to justify the functional similarity with the Na⁺ channel affecting scorpion α -toxins. However, significant structural differences such as the shorter size of the secondary structure elements might be responsible for the reduced toxicity of Crt when compared to other members belonging to the same family [12]. One example could be the reduced length of the α -helix that does not allow the formation of the cysteine-stabilized α -helix motif [72] common to most ion channel blocking polypeptides.

Similarly, the strong resemblance with the β -defensins fold [52–54], the conservation of some structural key residues as well as the arrangement of the disulfide bridges, might justify the common tendency to aggregate and interact with lipid membranes.

Note

A proposed structure of Crt, based on homology building and molecular dynamics simulations, has been published, recently [73]. The most significant difference between the theoretical 3D model and the NMR-derived structures is the lack of the N-terminal α -helix segment. A reason for that

could be the choice of the bovine β -defensin, BNBD12 [74], as a template.

Acknowledgements

The work was partly supported by CNR n. 99.02608.CT04, FIL and MIUR COFIN 2001 (A.S.). The Interfaculty Centre for Measurements (C.I.M.) of the University of Parma (Italy), the Department of Chemistry of the University of Padova (Italy), the EU NMR Large Scale Facilities in Frankfurt (UNIFRA LSF, Germany) and in Florence (PARABIO LSF, Italy) are gratefully acknowledged for the use of their equipment.

References

- Adams, M.D. & Swanson, G. (1996) Neurotoxins. *TINS* **19**, 2–36.
- Laure, C.J. (1975) The primary structure of crostamine. *Hoppe Seylers Z. Physiol. Chem.* **356**, 213–215.
- Giglio, J.R. (1975) Analytical studies on crostamine hydrochloride. *Anal. Biochem.* **69**, 207–221.
- Cheymol, J., Gonçalves, J.M., Bourillet, F. & Roch-Arveiller, M. (1971) A comparison of the neuromuscular action of crostamine and the venom of *Crotalus durissus terrificus* var. *crostaminicus* 1. Neuromuscular preparations *in situ*. *Toxicon* **9**, 279–286.
- Cheymol, J., Gonçalves, J.M., Bourillet, F. & Roch-Arveiller, M. (1971) A comparison of the neuromuscular action of crostamine and the venom of *Crotalus durissus terrificus* var. *crostaminicus* 2. Isolated preparations. *Toxicon* **9**, 287–289.
- Chang, C.C. & Tseng, K.H. (1978) Effect of crostamine, a toxin of south american rattlesnake venom, on the sodium channel of murine skeletal muscle. *Br. J. Pharmacol.* **63**, 551–559.
- Chang, C.C., Hong, S.J. & Su, M.J. (1983) A study on the membrane depolarization of skeletal muscles caused by a scorpion toxin, sea anemone toxin II and crostamine and the interaction between toxins. *Br. J. Pharmacol.* **79**, 673–680.
- Hong, S.J. & Chang, C.C. (1983) Potentiation by crostamine of the depolarizing effects of batrachotoxin, protoveratrine A and grayanotoxin I on the rat diaphragm. *Toxicon* **21**, 503–514.
- Vital-Brazil, O. & Fontana, M. D. (1993) Toxins as tools in the study of sodium channel distribution in the muscle fibre membrane. *Toxicon*, **31**, 1085–1098.
- Hong, S.J. & Chang, C.C. (1989) Use of geographutoxin II (μ -conotoxin) for the study of neuromuscular transmission in mouse. *Br. J. Pharmacol.* **97**, 934–940.
- Matavel, A.C.S., Ferreira-Alves, D.L., Beirão, P.S.L. & Cruz, J.S. (1998) Tension generation and increase in voltage-activated Na⁺ current by crostamine. *Eur. J. Pharmacol.* **348**, 167–173.
- Mancin, A.C., Soares, A.M., Andrião-escarso, S.H., Faça, V.M., Greene, L.J., Zuccolotto, S., Pela, I.R. & Giglio, J.R. (1998) The analgesic activity of crostamine, a neurotoxin from *Crotalus durissus terrificus* (South American rattlesnake) venom: a biochemical and pharmacological study. *Toxicon* **36**, 1927–1937.
- Cameron, D.L. & Tu, A.T. (1978) Chemical and functional homology of myotoxin a from prairie rattlesnake venom and crostamine from South American rattlesnake venom. *Biochem. Biophys. Acta* **532**, 147–154.
- Fletcher, J.E., Hubert, M., Wieland, S.J., Gong, Q. & Jiang, M. (1996) Similarities and differences in mechanisms of cardiotoxins, melittin and other myotoxins. *Toxicon* **34**, 1301–1311.
- Fox, J.W., Elzinga, M. & Tu, A.T. (1979) Amino acid sequence and disulfide bond assignment of myotoxin a isolated from the venom of prairie rattlesnake *Crotalus viridis viridis*. *Biochemistry* **18**, 678–684.
- Maeda, N., Tamiya, N., Pattabhiraman, T.R. & Russel, F.E. (1978) Some chemical properties of the venom of rattlesnake. *Crotalus viridis helleri*. *Toxicon* **16**, 431–441.

17. Bieber, A.L., McParland, R.H. & Becker, R.R. (1987) Amino acid sequences of myotoxins from *Crotalus viridis concolor* venom. *Toxicon* **25**, 677–680.
18. Samejima, Y., Aoki, Y. & Mebs, D. (1991) Amino acid sequence of a myotoxin from venom of the eastern diamondback rattlesnake (*Crotalus adamanteus*). *Toxicon* **29**, 461–468.
19. Bieber, A.L. & Nedelkov, D. (1997) Structural, biological and biochemical studies of myotoxin a and homologous myotoxins. *J. Toxicol. Toxin Rev.* **16**, 33–52.
20. Marion, D. & Wüthrich, K. (1983) Application of phase-sensitive two-dimensional correlated spectroscopy (COSY) for measurement of proton-proton spin-spin coupling constants. *Biochem. Biophys. Res. Commun.* **113**, 967–974.
21. Mareci, T.H. & Freeman, R. (1983) Mapping proton-proton coupling via double-quantum coherence. *J. Magn. Res.* **51**, 531–535.
22. Davis, D.G. & Bax, A. (1985) Assignment of complex ^1H -NMR spectra via two-dimensional homonuclear Hartman-Hahn spectroscopy. *J. Am. Chem. Soc.* **107**, 2820–2821.
23. Griesinger, C., Otting, G., Wüthrich, K. & Ernst, R.R. (1988) Clean TOCSY for ^1H spin system identification in macromolecules. *J. Am. Chem. Soc.* **110**, 7870–7872.
24. Jeener, J., Meier, B.H., Bachmann, P. & Ernst, R.R. (1979) Investigation of exchange processes by two-dimensional NMR spectroscopy. *J. Chem. Phys.* **71**, 4546–4553.
25. Piotto, M., Saudek, V. & Sklenar, V. (1992) Gradient-tailored excitation for single-quantum NMR spectroscopy of aqueous solutions. *J. Biomol. NMR* **2**, 661–665.
26. States, D.J., Haberkorn, R.A. & Ruben, D.J. (1982) A two-dimensional nuclear Overhauser experiment with pure absorption phase in four quadrants. *J. Magn. Res.* **48**, 286–292.
27. Wüthrich, K. (1986) *NMR of Proteins and Nucleic Acids*. John Wiley, New York.
28. Kim, Y. & Prestegard, J.H. (1989) Measurement of vicinal couplings from cross peaks in COSY spectra. *J. Magn. Reson.* **84**, 9–13.
29. Ludvigsen, S., Andersen, K.V. & Poulsen, F.M. (1991) Accurate measurements of coupling constants from two-dimensional nuclear magnetic resonance spectra of proteins and determination of ϕ -angles. *J. Mol. Biol.* **217**, 731–736.
30. Nilges, M., Clore, G.M. & Gronenborn, A.M. (1988) Determination of three-dimensional structures of proteins from inter-proton distance data by dynamical simulated annealing from a random array of atoms. Circumventing problems associated with folding. *FEBS Lett.* **239**, 129–136.
31. Laskowski, R.A., Rullmann, J.A., MacArthur, M.W., Kaptein, R. & Thornton, J.M. (1996) AQUA and PROCHECK-NMR: programs for checking the quality of protein structures solved by NMR. *J. Biomol. NMR* **8**, 477–486.
32. Koradi, R., Billeter, M. & Wüthrich, K. (1996) MOLMOL: a program for display and analysis of macromolecular structures. *J. Mol. Graphics* **14**, 51–55.
33. Dufton, M.J. & Hider, R.C. (1983) Conformational properties of the neurotoxins and cytotoxins isolated from Elapid snake venoms. *CRC Crit. Rev. Biochem.* **14**, 113–171.
34. Grognet, J.M., Menez, A., Drake, A., Hayashi, K., Morrison, I.E.G. & Hider, R.C. (1988) Circular dichroic spectra of elapid cardiotoxins. *Eur. J. Biochem.* **172**, 383–388.
35. Woody, R.W. (1994) Contribution of tryptophan side chains to the far-ultraviolet circular dichroism of proteins. *Eur. Biophys. J.* **23**, 253–262.
36. Hider, R.C., Drake, A.F. & Tamiya, N. (1988) An analysis of the 225–230 nm CD band of elapid toxins. *Biopolymers* **27**, 113–122.
37. Beltran, J.R., Mascarenhas, Y.P., Craievich, A.F. & Laure, C.J. (1990) SAXS study of the snake toxin α -crotamine. *Eur. Biophys. J.* **17**, 325–329.
38. Beltran, J.R., Mascarenhas, Y.P., Craievich, A.F. & Laure, C.J. (1985) SAXS study of structure and conformational changes of crotamine. *Biophys. J.* **47**, 33–35.
39. Hampe, O.G., Vozari-Hampe, M.M. & Gonçalves, J.M. (1978) Crotamine conformation effect of pH and temperature. *Toxicon* **16**, 453–460.
40. Hampe, O.G., Junqueira, N.O. & Vozari-Hampe, M.M. (1990) Polyacrylamide gel electrophoretic studies on the self association of crotamine: characterization and molecular dimension of *n*-mer species. *Electrophoresis* **11**, 475–478.
41. Wecker, K., Morellet, N., Bouaziz, S. & Roques, B.P. (2002) NMR structure of the HIV-1 regulatory protein Vpr in H_2O /trifluoroethanol. Comparison with the Vpr N-terminal (1–51) and C-terminal (52–96) domains. *Eur. J. Biochem.* **269**, 3779–3788.
42. Gagné, S.M., Tsuda, S., Li, M.X., Chandra, M., Smillie, L.B. & Sykes, B.D. (1994) Quantification of the calcium-induced secondary structural changes in the regulatory domain of troponin-C. *Protein Sci.* **3**, 1961–1974.
43. Slupsky, C.M. & Sykes, B.D. (1995) NMR solution structure of calcium-saturated skeletal muscle troponin C. *Biochemistry* **34**, 15953–15964.
44. Slupsky, C.M., Cyril, M.K., Reinach, F.C., Smillie, L.B. & Sykes, B.D. (1995) Calcium-induced dimerization of troponin C: mode of interaction and use of trifluoroethanol as a denaturant of quaternary structure. *Biochemistry* **34**, 7365–7375.
45. Endo, T., Oya, M., Ozawa, H., Kawano, Y., Giglio, J.R. & Miyazawa, T. (1989) A proton nuclear magnetic resonance study on the solution structure of crotamine. *J. Prot. Chem.* **8**, 807–815.
46. O’Keefe, M.P., Nedelkov, D., Bieber, A.L. & Nieman, R.A. (1996) Evidence for isomerization in myotoxin a from the prairie rattlesnake (*Crotalus viridis viridis*). *Toxicon* **34**, 417–434.
47. Richardson, J.S. (1981) The anatomy and taxonomy of protein structure. *Adv. Protein. Chem.* **34**, 167–339.
48. Wheeler, K.P., Watt, D.D. & Lazdunski, M. (1983) Classification of Na^+ channel receptors specific for various scorpion toxins. *Eur. J. Physiol.* **397**, 164–165.
49. Bontems, F., Roumestand, C., Gilquin, B., Menez, A. & Toma, F. (1991) Refined structure of Charybdotoxin: common motifs in scorpion toxins and insect defensins. *Science* **254**, 1521–1523.
50. Bruix, M., Jimenez, M.A., Santoro, J., Gonzales, C., Colilla, F.J., Mendez, E. & Rico, M. (1993) Solution structure of γ -1H and γ -IP thionins from barley and wheat endosperm determined by ^1H -NMR: a structural motif common to toxic arthropod proteins. *Biochemistry* **32**, 715–724.
51. Schibli, D., Hunter, H.N., Aseyev, V., Starner, T.D., Wiencek, J.M., McCray, P.B., Tack, B.F. & Vogel, H.J. (2002) The solution structures of human β -defensins lead to a better understanding of the potent bactericidal activity of HBD-3 against *Staphylococcus*. *J. Biol. Chem.* **277**, 8279–8289.
52. Hoover, D.M., Rajashankar, K.R., Blumenthal, R., Puri, A., Oppenheim, J.J., Chertov, O. & Lubkowski, J. (2000) The structure of human β -defensin-2 shows evidence of higher order oligomerization. *J. Biol. Chem.* **275**, 32911–32918.
53. Sawai, M.V., Jia, H.P., Liu, L., Aseyev, V., Wiencek, J.M., McCray, P.B., Ganz, T., Kearney, W.R. & Tack, B.F. (2001) The NMR structure of human β -defensin-2 reveals a novel α -helical segment. *Biochemistry* **40**, 3810–3816.
54. Hoover, D.M., Chertov, O. & Lubkowski, J. (2001) The structure of human β -defensin-1. *J. Biol. Chem.* **276**, 39021–39026.
55. Bloch, C. Jr, Patel, S.U., Baud, F., Zvelebil, M.J.J.M., Carr, M.D., Sadler, P.J. & Thornton, J.M. (1998) ^1H -NMR Structure of an Antifungal γ -Thionin Protein SI α 1: Similarity to Scorpion Toxins. *PROTEINS: Structure, Function, Genetics* **32**, 334–349.
56. Gordon, D., Martin-Eauclaire, M.F., Cestele, S., Kopeyan, C., Carlier, E., Khafifa, R., Pelhate, M. & Rochat, H. (1996) Scorpion

- toxins affecting sodium current inactivation bind to distinct homologous receptor sites on rat brain and insect sodium channels. *J. Biol. Chem.* **271**, 8034–8045.
57. Cestele, S. & Gordon, D. (1998) Depolarization differentially affects allosteric modulation by neurotoxins of scorpion α -toxin binding on voltage-gated sodium channels. *J. Neurochem.* **70**, 1217–1226.
58. Gordon, D. (1997) Sodium channels as target for neurotoxins. In *Toxins and Signal Transduction* (Gutman, Y. & Lazarowici, P., eds), pp. 119–149, Harwood. Academic Publishers, The Netherlands.
59. Fontecilla-Camps, J.C., Habersetzer-Rochat, C. & Rochat, H. (1988) Orthorhombic crystals and three-dimensional structure of the potent toxin II from the scorpion *Androctonus australis* Hector. *Proc. Natl Acad. Sci. USA* **85**, 7443–7447.
60. Housset, D., Habersetzer-Rochat, C., Astier, J.P. & Fontecilla-Camps, J.C. (1994) Crystal structure of toxin II from the scorpion *Androctonus australis* Hector refined at 1.3 Å resolution. *J. Mol. Biol.* **238**, 88–103.
61. Kharrat, R., Darbon, H., Rochat, H. & Granier, C. (1989) Structure/activity relationships of scorpion alpha-toxins. Multiple residues contribute to the interaction with receptors. *Eur. J. Biochem.* **181**, 381–390.
62. Zilberberg, N., Gordon, D., Pelhate, M., Adams, M.E., Norris, T.M., Zlotkin, E. & Gurevitz, M. (1996) Functional expression and genetic alteration of an alpha scorpion neurotoxin. *Biochemistry* **35**, 10215–10222.
63. Possani, L.D., Becerril, B., Delepierre, M. & Tytgat, T. (1999) Scorpion toxins specific for Na⁺ channels. *Eur. J. Biochem.* **264**, 287–300.
64. Li, H., Wang, D., Zeng, Z., Jin, L. & Hu, R. (1996) Crystal structure of an acidic neurotoxin from scorpion *Buthus martensii* Karsch at 1.85 Å resolution. *J. Mol. Biol.* **261**, 415–431.
65. Darbon, H., Jover, E., Couraud, F. & Rochat, H. (1983) α -scorpion neurotoxin derivatives suitable as potential markers of sodium channels. *Int. J. Pept. Prot. Res.* **22**, 179–186.
66. Zilberberg, N., Froy, O., Loret, E., Cestele, S., Arad, D., Gordon, D. & Gurevitz, M. (1997) Identification of structural elements of a scorpion α -neurotoxin important for receptor site recognition. *J. Biol. Chem.* **272**, 14810–14816.
67. El Ayeb, M., Bahraoui, E.M., Granier, C. & Rochat, H. (1986) Use of antibodies specific to defined regions of scorpion alpha-toxin to study its interaction with its site on the sodium channel. *Biochemistry* **25**, 6671–6678.
68. Tugarinov, V., Kustanovich, I., Zilberberg, N., Gurevitz, M. & Anglister, J. (1997) Solution structures of a highly insecticidal recombinant scorpion α -toxin and a mutant with increased activity. *Biochemistry* **36**, 2414–2424.
69. Rogers, J.C., Qu, Y., Tanada, T.N., Scheuer, T. & Catterall, W.A. (1996) Molecular determinants of high affinity binding of α -scorpion toxin and sea anemone toxin in the S3–S4 extracellular loop in domain IV of the Na⁺ channel α subunit. *J. Biol. Chem.* **271**, 15950–15962.
70. Ganz, T. & Lehrer, R.I. (1995) Defensins. *Pharmacol. Ther.* **66**, 191–205.
71. Harder, J., Bartels, J., Christophers, E. & Schroder, J.M. (1997) A peptide antibiotic from human skin. *Nature* **387**, 861.
72. Kobayashi, Y., Sato, A., Takashima, H., Kyogoku, Y., Lambert, P., Kuroda, H., Chino, M., Watanabe, T.X., Kimuka, T., Sakakibara, S. & Morodor, L. (1991) The cysteine stabilized α helix: a common structural motif of ion channel blocking neurotoxic peptides. *Biopolymers* **31**, 1213–1220.
73. Siqueira, A.M., Martins, N.F., De Lima, M.E., Diniz, C.R., Cartier, A., Brown, D. & Maigret, B. (2002) A proposed 3D structure for crotamine based on homology building, molecular simulations and circular dichroism. *J. Mol. Graph. Model.* **20**, 389–398.
74. Zimmermann, G.R., Legault, P., Selsted, M.E. & Pardi, A. (1995) Solution structure of bovine neutrophil β -defensin-12: the peptide fold of the β -defensins is identical to that of the classical defensins. *Biochemistry* **34**, 13663–13671.
75. Thompson, J.D., Higgins, D.G. & Gibson, T.J. (1994) CLUSTALW: improving the sensitivity of progressive multiple sequence alignment through sequence weighting, position-specific gap penalties and weight matrix choice. *Nucl. Acids Res.* **22**, 4673–4680.